

Optimized Design of a Planar Haptic Device Using Passive Actuators

Tae-Woo Kim^{*,**}, Chang-Hyun Cho^{*,**}, Mun-Sang Kim^{**} and Jae-Bok Song^{*}

^{*} Department of Mechanical Engineering, Korea University, Seoul, Korea
(Tel : +82-2-958-6724; E-mail: twkim@korea.ac.kr)

^{**} Intelligent Robotics Research Center, KIST, Seoul, Korea

Abstract: Passive Haptic Devices have more benefit than the active in Stability. But Apart from benefits, it shows poor performance in haptic display. The author proposed the passive FME(Force Manipulability Ellipsoid) which can graphically show force generating ability of a passive haptic device. In this paper, performance indexes for the force approximation and pseudo friction cone are obtained with the passive FME and an optimized planar device with the indexes is proposed. Based on the above theory, experiment is conducted.

Keywords: Haptic, Redundant Actuation, Passive FME, and optimization.

1. INTRODUCTION

Many devices have been developed for the realization of teleoperation or interface to a virtual reality so far. The application area of these devices covers a wide range (for example, medical instruments or entertainment instruments etc.) and the availability of the devices has been demonstrated. A haptic device is the one which let the human feel the kinesthetic or tactile sense in broad meaning. Haptic devices can be divided according to actuation methods. The one is a device using active actuator such as motor (e.g., SensAble Co.'s Phantom[1]), another is the device using passive actuator such as brake or clutch (e.g., P-TER [2]).

Since Passive haptic device uses energy dissipative actuator, it has superiority in the stability. Furthermore, since the ratio of toque to weight in actuator, lighter device can be constructed. However, passive haptic devices have a limitation in haptic display. It is impossible to represent forces of all directions due to the force generating mechanism of brakes. While previous researches addressed limitations of a passive haptic display, no one clearly claimed what the limitation is and which direction is possible to a given kinematic configuration. Thus design of a passive haptic device is very complicated and time consuming job. Moreover, one cannot guarantee performance of a newly design passive haptic device.

In this paper, we will propose a performance guaranteed passive haptic device. Cho et al. proposed so called the passive FME (Force Manipulability Ellipsoid) which is an analysis method of a passive haptic device based on FME [3]. With the passive FME, we can clearly understand what the limitations are and build performance indexes, which leads to an optimized design of a passive haptic device. Better performance is guaranteed by the optimization:

- Minimized force approximation angles during haptic display
- Capability of avoiding pseudo friction cones.

The rest of this paper is organized as follows. The passive FME is briefly introduced in section 2. In section 3, Performance indexes are proposed and an optimization is conducted with the indexes. Section 4 denotes a control method which selects brakes to be actuated for avoiding the pseudo friction cone. Experiment results are presented in section 5 and finally in section 6, conclusion is drawn.

2. THE PASSIVE FME

It is generally known that a passive actuator can generate a torque only against rotation of its shaft. From this well known fact, constraint equations based on the Karnopp's stick-slip model can be acquired with considering haptic display [4].

Slip mode ($\dot{\theta} \neq 0$)

$$\tau_c = \begin{cases} -\text{sgn}(\dot{\theta})|\tau_d| & \text{if } \text{sgn}(\dot{\theta}) \neq \text{sgn}(\tau_d) \\ 0 & \text{else} \end{cases} \quad (1a)$$

Stick mode ($\dot{\theta} = 0$)

$$\tau_c = \begin{cases} -\tau_h & \text{if } \text{sgn}(\tau_h) \neq \text{sgn}(\tau_d) \\ 0 & \text{else} \end{cases} \quad (1b)$$

where τ_d is the desired torque required for haptic display (i.e., force reflection) and τ_h is the hand torque input to the device by a human operator. And $\dot{\theta}$ is the joint velocity, and τ_c is the control torque generated by the brake. The control torque is created in the direction opposite to either its shaft rotation in Eq. (1a) or the external hand torque acting on its shaft in Eq. (1b). Note that if a desired torque has the same sign as a joint velocity or a hand torque, the brake should be released (i.e., $\tau_c = 0$) to avoid producing a brake torque which is against the user's intention. In this paper Eq. (1) will be termed as the passive constraint.

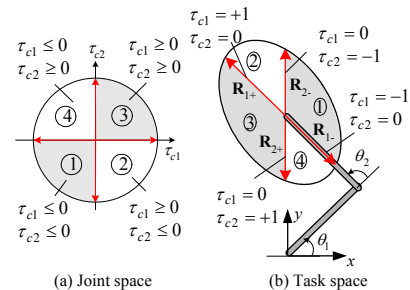


Fig. 1 A set of passive FMEs ($\theta_1 = 45^\circ$, $\theta_2 = 90^\circ$, $l_1 = l_2 = l$).

Possible sets of joint torque can be acquired by Eq. (1) as shown in Fig. 1(a). Thus each region in Fig. 1(a) represents the passive region I in the joint space and is then mapped into the corresponding region in task space by $\tau = \mathbf{J}(\mathbf{q})^T \mathbf{F}$ as

illustrated in Fig. 1(b). In passive haptic devices, the joint torque is closely related to the joint velocity by the passive constraint given by Eq. (1). Referring to Eq. (1), for example, only joint torques of $\tau_{c1} \leq 0$ and $\tau_{c2} \leq 0$ are available in region 1, if $\dot{\theta}_1 > 0$ and $\dot{\theta}_2 > 0$. When $\dot{\theta}_1 > 0$ and $\dot{\theta}_2 = 0$, for instance, $\tau_{c1} \leq 0$ but τ_{c2} is determined only by τ_{h2} (see Eq. (1b)). From all possible combinations of joint velocities, we observed that control torques can be represented by 4 regions in Fig. 1(a) regardless of whether the joints are in either the slip mode or the stick mode.

A set of passive FMEs can be drawn by mapping c in joint space into the end-effector force \mathbf{F}_c in task space using the Jacobian mapping of $\boldsymbol{\tau} = \mathbf{J}(\mathbf{q})^T \mathbf{F}$. Thus each region in Fig. 1(a) is mapped into each corresponding passive FME illustrated in Fig. 1(b) which represents a set of passive FMEs. Each passive FME is delimited by four reference forces \mathbf{R}_{1+} , \mathbf{R}_{1-} , \mathbf{R}_{2+} , and \mathbf{R}_{2-} , where \mathbf{R}_i denotes the end-effector force when only brake i is applied (i.e., $\tau_{ci} \neq 0$) with the other brakes released. For example, if $\tau_{c1} > 0$ (or $\tau_{c1} < 0$) with $\tau_{c2} = 0$, then force \mathbf{R}_{1+} (or \mathbf{R}_{1-}) is generated. Likewise, \mathbf{R}_{2+} (or \mathbf{R}_{2-}) is generated for $\tau_{c2} > 0$ (or $\tau_{c2} < 0$) with $\tau_{c1} = 0$. Note that the Jacobian and thus reference forces change as the manipulator moves.

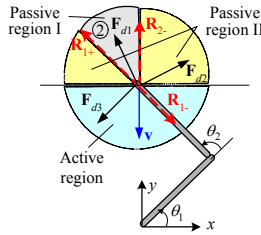


Fig. 2 Force approximation ($\theta_1 = 45^\circ$, $\theta_2 = 90^\circ$, $l_1 = l_2 = l$).

Consider an example in Fig. 2 for detailed analysis. Suppose that the end-effector P is moving in the $-y$ direction, in which $\dot{\theta}_1 < 0$ and $\dot{\theta}_2 > 0$. Hence, the brakes can generate a force only in passive FME 2 (i.e., $\tau_{c1} > 0$ and $\tau_{c2} < 0$) because of the passive constraint. Note in passive FME 2 that $\tau_{c1} \dot{\theta}_1 < 0$ and $\tau_{c2} \dot{\theta}_2 < 0$, and thus $\boldsymbol{\tau} \cdot \dot{\mathbf{q}} = \tau_{c1} \dot{\theta}_1 + \tau_{c2} \dot{\theta}_2 < 0$ in Eq. (1). Since passive FME 2 belongs to passive region I, the desired force \mathbf{F}_{d1} in this region can be accurately displayed by a resultant force of \mathbf{R}_{1+} and \mathbf{R}_{2-} . On the other hand, the desired \mathbf{F}_{d2} belonging to passive region II needs to be represented by a combined force of \mathbf{R}_{2-} and \mathbf{R}_{1-} in Fig. 1, but generation of \mathbf{R}_{1-} requires $\tau_{c1} < 0$ which violates the passive constraint of $\tau_{c1} \cdot \dot{\theta}_1 \leq 0$. Therefore, \mathbf{F}_{d2} cannot be accurately displayed but only approximately by the nearest available force \mathbf{R}_{2-} alone, which is called *force approximation* in passive haptic devices. Finally, the desired force \mathbf{F}_{d3} cannot be displayed at all since it belongs to the active region of $\mathbf{F} \cdot \mathbf{V} > 0$. Consequently, there exist regions in which the desired force cannot be displayed or can be displayed only approximately in the case of passive haptic devices, and these regions can be found by the passive FME analysis.

The so-called *pseudo friction cone* will be used to analyze the phenomenon of the deadlock of the end-effector in some cases. It is convenient to introduce the concept of a friction cone for analysis of the end-effector motion of a haptic device on the virtual surface. Since frictionless surface is usually assumed, however, the motion is stuck not by friction but by

other phenomenon which will be discussed below.

Figure 3 is an example of haptic display on a virtual wall which has a unit normal vector \mathbf{n} in the same direction as the y axis. For simplicity of analysis, the initial state of the passive haptic device in Fig. 3 will be assumed that all joint velocities are initially zero. Because the virtual wall is assumed to have no friction, the desired force \mathbf{F}_d is in the same direction as that of \mathbf{n} . A force \mathbf{F}_h applied by a human operator at the end-effector is assumed to be given to allow motion along the surface while maintaining contact with the wall. $Q_{i\pm}$ in Fig. 3 is a possible path of the end-effector when brake i is fully activated (or locked) and '+' indicates the link rotation in the positive direction. Hence the end-effector location at the next instant is determined by a linear combination of Q_1 and Q_2 at the current instant. When the user applies \mathbf{F}_{ha} to move the end-effector to the right, the paths Q_{1-} and/or Q_{2-} will be induced, thus resulting in penetration into the wall. Thus the end-effector is likely to be stuck at the next instant. However, when the user applies \mathbf{F}_{hb} to move the end-effector to the left, the paths Q_{1+} and/or Q_{2+} will be invoked, thus leading to no penetration into the wall. This enables the motion along the surface at the next instant.

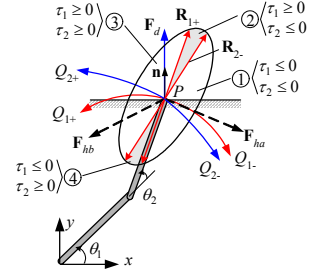


Fig. 3 Example of haptic display

In this example, the end-effector is stuck when the desired force \mathbf{F}_d is in passive FME 3 ($\tau_{d1} > 0$, $\tau_{d2} > 0$) and the user applies the force \mathbf{F}_{ha} in passive FME 1 ($\tau_{ha1} < 0$, $\tau_{ha2} < 0$) which is located on the opposite side of passive FME 3. This example can be generalized that a pseudo friction cone coincides with the passive FME on the opposite side of the passive FME where a desired force exists. If the user hand force belongs to the pseudo friction cone, then the end-effector is stuck regardless of the user's intention of moving it on the surface. It is noted that all four passive FMEs can be a pseudo friction cone depending on the direction of the desired force. As in the friction cone, the angle of the pseudo friction cone can be used as a measure of quality for haptic display in path guidance. Of course, the smaller the angle is, the better the quality is.

2. OPTIMIZED DESIGN OF DEVICE

2.1 Performance Index

Performance indexes are induced for passive haptic device's limitations such as force approximation and pseudo friction cone. Fig.4 shows schematic of approximation in 2DOF planar passive Haptic Device. \mathbf{F}_d is the force to represent repulsive force, and the possible range of force reflection is gray one. An approximation region is quantitatively represented by $\alpha_1 + \alpha_2$.

$$\alpha_1 + \alpha_2 = \pi - \beta_1 \quad (2)$$

where β_1 is the angle between reference force \mathbf{R}_1 and \mathbf{R}_2 , and for the remaining passive FMEs, the approximation range can be also found. The value is calculated by (2). The capability for approximation is determined by summation of all approximation regions for all possible passive FMEs in a given configuration. So following performance index can be defined as.

$$P_a = \sum_{i=1}^n (\pi - \beta_i)^2 \quad (3)$$

where n is number of passive FME. Since Eq.(3) corresponds to a specific position, it is needed to consider for the entire workspace. So following equation can be defined as

$$GP_a = \frac{1}{V} \int \sum_{i=1}^n (\pi - \beta_i)^2 \quad (4)$$

and discrete form of Eq. (4) is as follows.

$$GP_a = \frac{1}{m} \sum_{j=1}^m [P_a]_j = \frac{1}{m} \sum_{j=1}^m \left[\sum_{i=1}^n (\pi - \beta_i)^2 \right]_j \quad (5)$$

where $[P_a]_j$ means local performance index measured in j th configuration, m is total number of measured point in workspace.

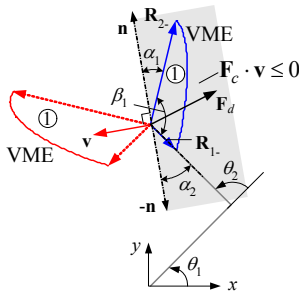


Fig. 4 Approximation schematic in 2DOF planar passive Haptic Device

The limitation of PFC (Pseudo Friction Cone) is related with the size of β_i . Thus local performance index of PFC is defined as follows.

$$P_f = [\max(\beta_1, \dots, \beta_n)]^2 \quad (6)$$

If optimization is conducted by Eq.(6), it comes to Min-Max problem. Since it is minimized to the worst case, it causes to lessen the deviation of all β_i . Discrete form of Eq. (6) is as follows.

$$GP_f = \frac{1}{m} \sum_{j=1}^m [\max(\beta_1, \dots, \beta_n)]^2 \quad (7)$$

2.2 Optimized Design

Since the number of joints is five and the number of brakes is four, five combinations of brakes are possible. Brake 1 & 2 can be installed in bottom position of device in direct, but brakes for other joints apply tendon-driven method to lessen

the weight of link part. In 5bar link, each link length and two joint angles determine the remaining angles. So link lengths and reduction ratios can be used for optimization parameters. To reduce the number of parameters, link length is represented by ratio to length of link 5 [5].

$$\mathbf{X} = [l_1/l_5 \quad l_2/l_5 \quad l_3/l_5 \quad l_4/l_5 \quad k_1 \quad k_2 \quad k_3 \quad k_4]^T \quad (8)$$

$$\mathbf{X} = [\gamma_1 \quad \gamma_2 \quad \gamma_3 \quad \gamma_4 \quad k_1 \quad k_2 \quad k_3 \quad k_4]^T \quad (9)$$

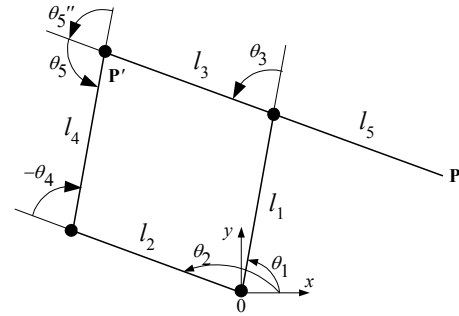


Fig. 5 5bar Linkage.

In the above performance Indexes, because GP_f uses Max function, it will be assumed that non-linearity and discontinuity exist. Furthermore it is needed to limit parameters properly with consideration on the working volume and device construction. So optimization comes to be constrained optimizing problem and following conditions are considered.

$$V_{\min} \leq V \quad (10)$$

$$\gamma_{\min} \leq \gamma_i \leq \gamma_{\max} \quad (11)$$

$$k_{\min} \leq k_i \leq k_{\max} \quad (12)$$

Equation (10) (or (11)) denotes constraint for working volume (or link length). Equation (12) is for the reduction ratio. While k_i is more than 1.0, it means acceleration. So k_{\max} is set to be 1, and k_{\min} is set to be real limitation in the device construction.

In addition to the above performance indexes, it is needed to consider the capacity of brake torques to be sufficient to design specification. So more small total brake torque, lighter device weight is. Finally total number of performance indexes is three. Thus a proper combination of the indexes is needed.

When considering performance indexes and constrained conditions, optimization is the problem of multi-objective non-linear optimizing. Firstly, in multi-objective problem, utility function method is selected with the results of convergence test [6]. Secondly, in constrained non-linear optimizing problem, exterior penalty function method is used. Multi-modal problem has the multiple local minimums and therefore various initial conditions are set so to find a local minimum close to initial condition. The minimum of local minimums comes to be global minimum.[7,8]

The torque ratio in Table 1 is a ratio of a pre-defined torque to a calculated torque. At table 1, examining each value of performance indexes, a specific index is good but others are poor according to combinations. This result comes from the multi-objective problem, so all indexes cannot show good performance due to negotiation between the indexes. Therefore to find best combination, it is reasonable to set priority for calculated results. At the table 1, the more in left

side index is, the more high priority is. For the moment, 2 italic-typed combinations are selected. Examining Max approximation angle and Max virtual friction cone, it can be shown that very large difference exists. Max approximation angle of 2-3-4-5 combination is 3-times as large as 1-2-3-4, and 2-3-4-5 combination must have 2-stage tendon driven method to actuating brake 5. So 1-2-3-4 combination is suitable in performance and construction.

Table 1 Optimizing results for the five combinations.

	GP_a	GP_f	Tor. ratio	Max App. Angle	Min App. Angle	Max PFC	Min PFC
2-3-4-5	1.309	0.321	1.691	171°	3.8°	112.4°	0.8°
1-3-4-5	3.289	0.336	1.402	114°	2.0°	89.6°	13.3°
1-2-4-5	2.970	0.207	1.454	151°	7.7°	93.8°	8.2°
1-2-3-5	1.727	0.576	1.657	151°	0.3°	118.7	5.7°
1-2-3-4	1.333	0.046	1.784	62°	14.0°	78.6°	0.8°

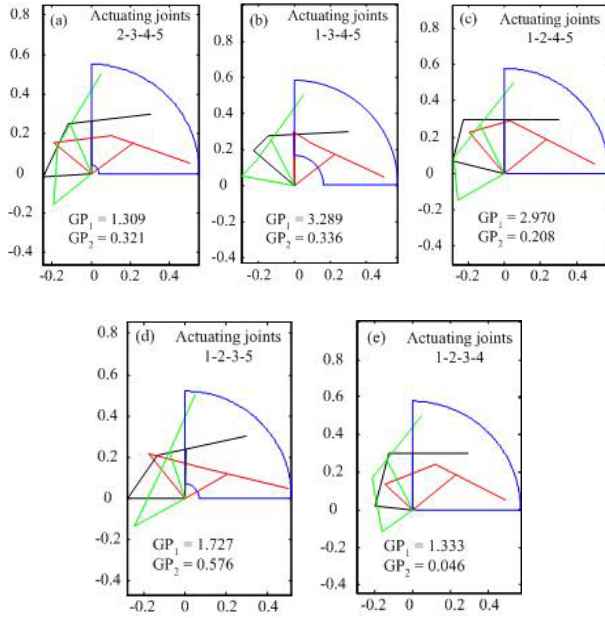


Fig. 6 Optimized 5bar for the five combinations with working volume.

3. CONTROL

Reference forces should be calculated to set passive FME as shown in section 2.

$$\mathbf{F} = \mathbf{J}(\mathbf{q})^{-T} \boldsymbol{\tau} \quad (13)$$

$$(\mathbf{J}^T)^{-1} = [\mathbf{J}_1 | \mathbf{J}_2 | \mathbf{J}_3 | \mathbf{J}_4] \quad (14)$$

With Eq. (14), reference forces can be calculated as follows.

$$\mathbf{R}_{i+} = \mathbf{J}_i, \mathbf{R}_{i-} = -\mathbf{J}_i \quad (15)$$

where i is the joint number, \mathbf{J}_i is i th row vector of $(\mathbf{J}^T)^{-1}$. For example, \mathbf{R}_{1+} can be calculated with $t_{c1} = 1, t_{c2} = t_{c3} = t_{c4} = 0$. In the meantime, while position of manipulator changes, manipulator Jacobian also changes. Reference forces changes

consequently. In passive haptic device using brake, joint space has the following condition.

$$\tau_{ci} \cdot \dot{\theta}_i \leq 0 \quad (16)$$

, so a desired force to be displayed is only possible by reference forces that satisfies Eq. (16).

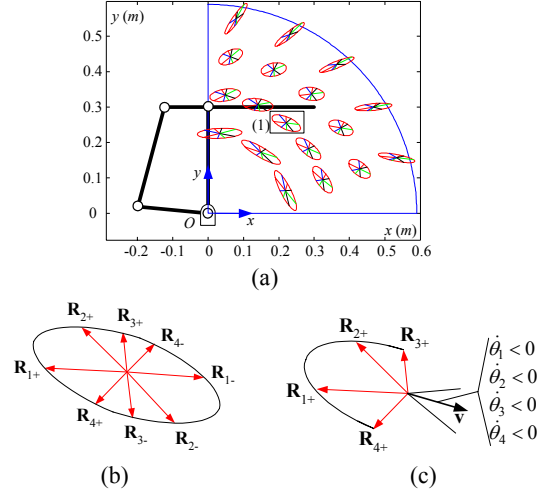


Fig. 7 Passive FMEs of the optimized 5bar mechanism



Fig. 8 Brake Torque Generation Flow chart

Optimized 5bar linkage is showed in Fig. 7. Fig. 7(a) represents passive FMEs in the working volume and Fig. 7(b) denotes a magnified view of area (1) in the Fig. 7(a). Fig. 7(c)

shows possible reference forces in passive FME for a given endpoint velocity. Whole area is divided to 3 parts by brake actuation and limitation on the pseudo friction cone can be solved by selective actuation. The Fig.8 shows brake torque generation process for force display.

4. EXPERIMENT

4.1 Experimental setup

The proposed device equipped with 4 electric brakes shown in Fig.9 was constructed for experiments. Every joints are actuated by tendon-drive mechanism. Brakes are mounted at the base and convey the torque through pulleys. Placing brakes at the base has an advantage of reducing the mass of the moving part. The F/T sensor is mounted at the handle to measure the hand force provided by the user. The directions of exerting hand torques are calculated with the measured hand force input by using $\tau = J(q)^T F$ so as to draw a passive FME even though a joint velocity is zero(i.e., the stick mode). Rotational motion of each brake is sensed by the optical encoder mounted on the brake axis.

In the experiments, the brake control is conducted at a rate of 1kHz.

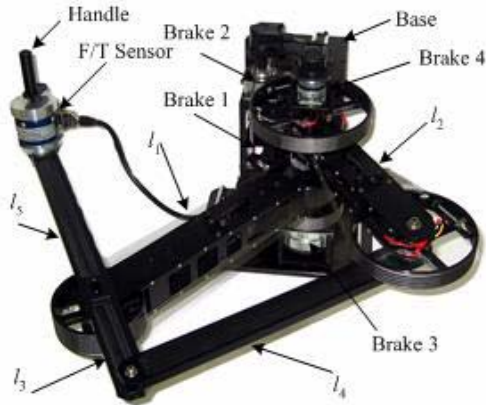


Fig. 9 The proposed device

4.2 Results

Experiments are conducted for vertical virtual wall. Its stiffness is assumed to be $10^3 N/m$ and it has no damping or frictional effect. Since surface normal is $-x$ direction, the direction of desired force is always $-x$ direction.

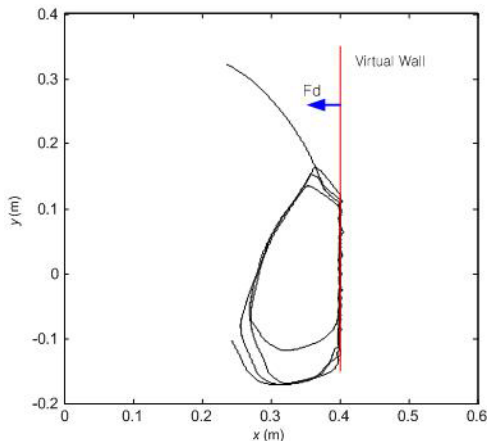


Fig. 10 Wall display test

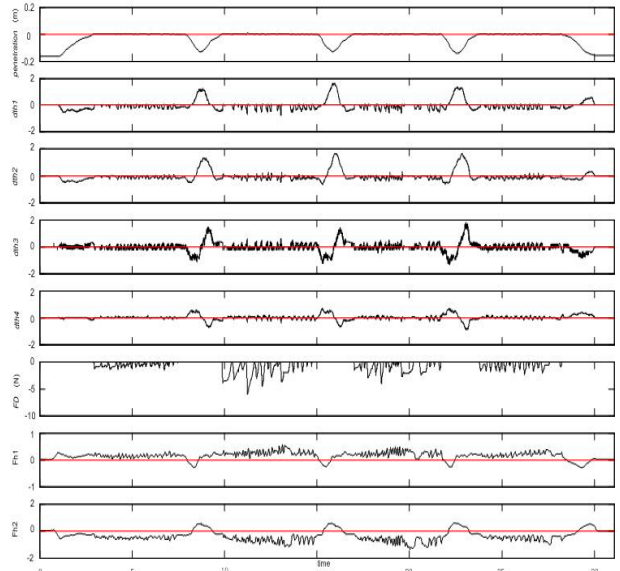


Fig. 11 Penetration, joint velocity, F_d , and F_h

Figure 10 shows wall following trajectory. Figure 11 and 12 show data obtained from the wall display test. Desired torques are calculated with F_d by Eq. (13). In this test, brake 1 & 2 are used selectively according to the control method which is designed to avoid the PFC. Torques measured with F/T sensor are used for determining brake modes (i.e., stick or slip).

Fig.13 shows available reference force set at a specific instant ($= 11.754sec$). $F_d (= -2.921N)$ exist in the PFC (pseudo friction cone). If operator wants to let the end effector move along the wall, reference forces outside PFC are selected to avoid the sticking problem. In this case, brake 2 is selected by the control method, which means that the desired torque of brake 2 ($Br2T$) is set to $-1.251Nm$ and the others are set to zero. As a result, human can feel as if real wall exist at that position and also move the end-effector without sticking. It is noted that the end-effector will be stuck, if the control method does not applied (i.e., PFC is activated).

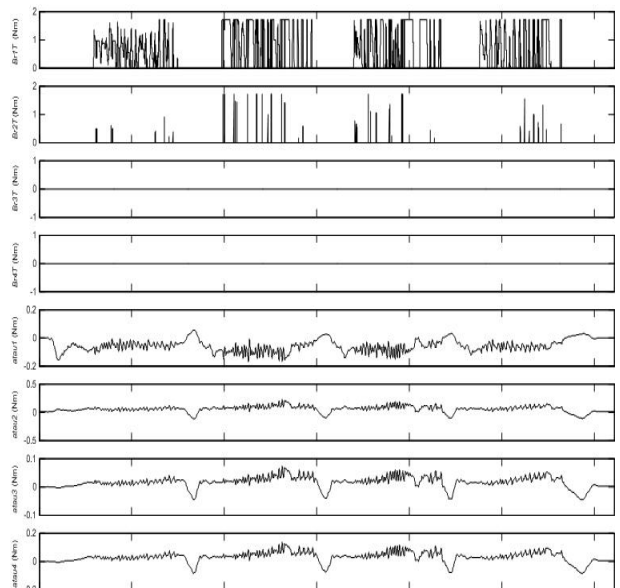


Fig. 12 Desired torque and measured torque

[8] W. Spendley, G. R. Hext, and F. R. Himsworth, "Sequential Application of Simplex Design in Optimization and Evolutionary Operation," *Technometrics*, Vol. 4, pp. 441, 1962.

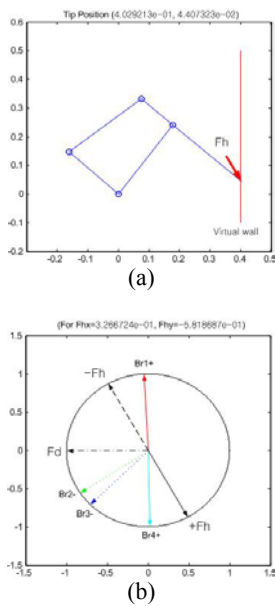


Fig. 13 Reference force set at a location

5. CONCLUSION

Based on the passive FME analysis, we proposed an optimized planar device to the limitation of the force approximation and pseudo friction cone. A control method is presented for avoiding the pseudo friction cone in runtime. Thus the device can move along the surface without sticking behavior, which is verified by experiments. In experimental device, frictional brakes are used for generating braking torques. However they have nonlinearities such as a hysteresis. Thus a control method of brake considering the nonlinearity should be implemented to achieve accurate torque generation.

ACKNOWLEDGMENTS

The authors gratefully acknowledge the contribution of Beom-Seop Kim.

REFERENCES

[1] SensAble Technologies, <http://www.sensable.com/>

[2] H. Davis, W. Book, "Torque control of a Redundantly actuated Passive Manipulator," *Proc. Of the American Control Conference*, pp. 959~963, 1997.

[3] C. H. Cho, M. S. Kim and J. B. Song, "Performance analysis of a 2-link haptic device with electric brakes," *Proc. of 11th Symposium on Haptics*, pp. 47 -53, 2003.

[4] D. Karnopp, "Computer Simulation of Stick-Slip Friction in Mechanical Dynamic System," *ASME Journal of Dynamic Systems, Measurement, and Control*, Vol. 107, pp. 100~103, 1985.

[5] Lee, S. H., B. J. Yi, S. H. Kim, and Y. K. Kwak, "Optimization of the Antagonistic Stiffness Characteristic of a Five-bar Mechanism with Redundant Actuation," *Proc. Of Int. Conf. On Intelligent Robots and System IROS 1999*, pp. 1386~1392, 1999.

[6] Rao, S. S., *Engineering Optimization: Theory and practice 3rd Ed*, Wiley & Sons Inc., 1996.

[7] Nelder, J.A. and R. Mead, "A Simplex Method for Function Minimization," *Computer J.*, Vol.7, pp 308-313, 1965.